Mecánica Computacional Vol. XXI, pp. 462–475
S. R. Idelsohn, V. E. Sonzogni and A. Cardona (Eds.)
Santa Fe–Paraná, Argentina, October 2002

COMPUTING PAST CYLINDER FLOWS

Marcela A. Cruchaga[*], Norberto M. Nigro[†], Mario A. Storti[†] and Diego J. Celentano[*]

[*]Departamento de Ingeniería Mecánica
Universidad de Santiago de Chile
Av. Bdo. O´Higgins 3363
Santiago, Chile
e-mail: dcelenta@lauca.usach.cl; mcruchag@lauca.usach.cl

[†]Centro Internacional de Métodos Computacionales en Ingeniería (CIMEC)
Universidad Nacional del Litoral
Güemes 3450
3000 Santa Fe, Argentina
e-mail: nnigro@intec.unl.edu.ar; mstorti@intec.unl.edu.ar

Key words: flow past cylinders, finite element analysis, parallel computations in PC.

Abstract. *In this work a numerical study of flow past circular cylinders is presented. The simulations are carried out using two different computational codes both written in the context of the finite element method. One of them is an optimized code developed in the framework of PETSc libraries able to run in parallel using an interconnected system of personal computers. The other one is a conventional serial code. The objectives of this analysis are: to check the capabilities of a cluster composed of four nodes, to test the performance of the proposed codes in the analysis of highly time dependent problems, to perform comparisons with results obtained by using different convergence strategies and to verify the behavior of alternative solvers.*

1 INTRODUCTION

The study of flows around bodies is of interest in aircraft industry, car design or bridges flow resistance evaluation as examples of engineering applications where a properly prediction of drag and lift forces is required. In particular, simulations of flow past circular cylinders have been extensively proposed with different objectives [1-14]. From the numerical point of view it is an important test to check the performance of computational codes in highly time dependent problems. Additionally, it provides valuable information about changes in the flow pattern when different conditions are considered in wind channels, e.g. the influence of the relative distance between walls or inlet/outlet sections respect to the body position. In the framework of the finite element method, several efforts have been devoted to develop consistent incompressible Navier-Stokes flow formulations aimed at analyzing this kind of large-scale/long-term applications [1-22]. More recently, in order to optimize the use of computational resources, specific algorithms have been designed to work in parallel architectures [21,22]. From the computational standpoint, it does not only imply an adequate use of interconnected environments but also the development of appropriate codes able to be employed in such systems improving the performance of the numerical analysis.

In the present work past cylinder flows are analyzed using two different codes involving different finite element formulations and distinct computational structures. One of them, named "PETSc-FEM" [23], is a parallel version of the formulation presented in [4,6,22] written within the context of MPI routines and PETSc scientific libraries. In this framework, standard GMRES [22-25] and IISD [23] solvers have been implemented. In particular, the Interface-Iterative/Subdomain-Direct method (IISD) is a hybrid solver scheme based on domain decomposition that uses a direct solver inside each subdomain and an iterative solver on the interface between subdomains. The subdomain partition can be done either at processor level or in one processor making this strategy extensible to scalar computations. Depending on the number of chosen subdomains, it is possible to cover the alternatives ranging from pure direct methods to full iterative algorithms. This strategy enhances the convergence rate and it can be seen as a parallel direct method [23]. Moreover, PETSc-FEM can also run as a serial code with an improved LU solver [23]. On the other hand, the second program is a serial code based on a generalized streamline operator technique presented in [15-17] which uses a standard direct (skyline) solver.

The aim of this work is twofold: to validate the numerical predictions in flow past cylinder simulations and, besides, to analyze the performance of different solvers which is a crucial aspect in large-scale/long-term computations. To this end, a comparison between the results provided by both codes and with those reported in the literature are presented together with some measurements related to computational efficiency. The parallel code was installed in an interconnected system of four personal computers (Pentium IV, 400 Mhz) running in RedHat Linux 7.1. The serial code also works in this architecture. The study is performed for a Reynolds number of 100 showing evolutions of drag and lift coefficients, velocity and pressure time histories at certain points of the domain and computational times obtained using different methodologies and strategies. A brief description related to numerical aspects of both codes used is presented in Section 2. The modeling is reported in Section 3 and, finally,

we present the concluding remarks.

2 FINITE ELEMENT FORMULATIONS

The flow past cylinder analyzed is governed by the transient incompressible Navier-Stokes equations written in cartesian coordinates as:

- equation of motion:

$$\rho \dot{\mathbf{v}} + \rho(\mathbf{v}\cdot\nabla)\mathbf{v} + \nabla p - \nabla\cdot(2\mu\boldsymbol{\varepsilon}) = \rho\mathbf{b} \qquad in \quad \Omega\times \mathrm{Y} \tag{1}$$

- continuity equation:

$$\nabla\cdot\mathbf{v} = 0 \qquad in \quad \Omega\times \mathrm{Y} \tag{2}$$

together with adequate boundary and initial conditions. In these equations, standard notation is used: Ω is an arbitrary open bounded domain with smooth boundary Γ and Y is the time interval of interest (t∈Y). Moreover, ρ is the density, μ is the dynamic viscosity, **v** is the velocity vector, p is the pressure, **b** is the specific body force vector and **ε** is the rate of deformation tensor. The symbol ∇ denotes the spatial gradient operator and the dot over a variable represents its time derivative.

2.1 Weak form obtained from scalar upwinding coefficients

In the context of the finite element analysis, the integral form of the differential system of equations (1)-(2) can be obtained using a streamline upwinding Petrov-Galerkin technique plus pressure stabilization terms and a Galerkin least squared form for the incompressibility constraint [4,6,22]. The corresponding weak form can be described as follows:

$$\int_{\Omega}\mathbf{N}_{\mathrm{V}}\cdot\left[\rho\dot{\mathbf{v}}+\rho(\mathbf{v}\cdot\nabla)\mathbf{v}+\nabla p-\nabla\cdot(2\mu\boldsymbol{\varepsilon})-\rho\mathbf{b}\right]\partial\Omega+\int_{\Omega}\mathbf{N}_{\mathrm{p}}\nabla\cdot\mathbf{v}\,\partial\Omega$$
$$+\sum_{n=1}^{n_{el}}\left[\tau^{1}_{mom}(\mathbf{v}\cdot\nabla)\mathbf{N}_{\mathrm{V}}\right]\left[\rho\dot{\mathbf{v}}+\rho(\mathbf{v}\cdot\nabla)\mathbf{v}+\nabla p-\nabla\cdot(2\mu\boldsymbol{\varepsilon})-\rho\mathbf{b}\right]\partial\Omega$$
$$+\sum_{n=1}^{n_{el}}\left[\tau^{2}_{mom}\nabla\mathbf{N}_{\mathrm{p}}\right]\left[\rho\dot{\mathbf{v}}+\rho(\mathbf{v}\cdot\nabla)\mathbf{v}+\nabla p-\nabla\cdot(2\mu\boldsymbol{\varepsilon})-\rho\mathbf{b}\right]\partial\Omega$$

$$+\sum_{n=1}^{n_{el}}\left[\tau_{cont}\nabla\cdot\mathbf{N}_{\mathbf{V}}\right]\left[\nabla\cdot\mathbf{v}\right]\partial\Omega+\int_{\Gamma}\mathbf{N}_{\mathbf{V}}\cdot\left[BC\right]\partial\Gamma=0 \tag{3}$$

where $\mathbf{N_V}$ and $\mathbf{N_p}$ are the basis (shape functions) of the discrete velocity and pressure spaces respectively. As usual, the domain Ω is split into a collection of n^{el} finite element domains Ω^{el}. Moreover, the variables **v** and p are described in the discrete space (no index notation is used for simplicity). Notice that in the first term, which belongs to the standard Galerkin formulation, no order reduction is performed for the viscous stress tensor. The last term represents the boundary conditions (BC) either Dirichlet or Neumann type. Several definitions of the upwinding parameters τ^1_{mom}, τ^2_{mom} and τ_{cont} have been consistently proposed in the bibliography. In the present work, two different set of expressions for such coefficients are adopted. The first one is taken from [4,6,22] and they read as:

$$\tau^1_{mom}=\left[\left(\frac{2}{\Delta t}\right)^2+\left(\frac{2\|\mathbf{v}\|}{h}\right)^2+9\left(\frac{4\mu}{h^2\rho}\right)^2\right]^{-\frac{1}{2}} \tag{4}$$

$$\tau^2_{mom}=\frac{\tau^1_{mom}}{\rho} \tag{5}$$

$$\tau_{cont}=\rho\frac{h}{2}\|\mathbf{v}\|f(R_e)\qquad with\quad f(R_e)=\begin{cases}\dfrac{R_e}{3} & R_e\le 3\\[2ex] 1 & R_e>3\end{cases} \tag{6}$$

where $R_e=\dfrac{\rho\|\mathbf{v}\|h}{2\mu}$ is the elemental Reynolds number and h is a characteristic element length. The definition of h introduces additional discussions (see [4,6,22] and references therein for further details).

A second choice for the upwinding coefficients can be considered as [18]:

$$\tau^1_{mom}=\begin{cases}0 & if\ R_e=0\\[2ex] \dfrac{\alpha_1 h}{2\|\mathbf{v}\|}f(R_e) & if\ R_e>0\end{cases} \tag{7}$$

$$\tau_{mom}^2 = \begin{cases} \dfrac{\alpha_2 h^2}{2\mu} & if\ R_e = 0 \\ \dfrac{\alpha_2 h^2}{2\mu} - \left(\dfrac{\alpha_2 h^2}{2\mu} - \dfrac{\alpha_1 h}{2\|\mathbf{v}\|\rho} \right) f(R_e) & if\ R_e > 0 \end{cases} \tag{8}$$

$$\tau_{cont} = \rho \frac{h}{2} \|\mathbf{v}\| f(R_e) \tag{9}$$

where $f(R_e)$ is the well known one-dimensional optimal upwinding function $f(R_e) = coth(R_e) - 1/R_e$ while α_1 and α_2 are coefficients that depend on the finite element topology (with values of 0.5 and 0.11, respectively, for 2D isoparametric four-noded elements). In the numerical simulations we use the finite element formulation derived from equation (3) including definitions given by equations (4)-(6) assuming no time-step dependency and null τ_{cont} due to the low Reynolds number analyzed. This methodology is identified as FEM1 in this work. A second formulation, called FEM2 in the present paper, is obtained from equation (3) with upwinding coefficients defined by equations (7)-(9) also considering $\tau_{cont} = 0$.

2.2 Weak form obtained through a generalized streamline operator

The basic formulation described by the residual form of equations (1)-(2) can be written in a compact manner as a generalized convection-diffusion system for n_{dim}-dimensional problems (n_{dim} being the spatial dimension) using indicial notation as [15-17]:

$$\mathbf{R}(\mathbf{U}) \equiv \mathbf{M}\,\dot{\mathbf{U}} + \mathbf{A}_n \nabla_n \mathbf{U} - \nabla_j (\mathbf{K}_{jn} \nabla_n \mathbf{U}) - \mathbf{F} = \mathbf{0} \quad in \quad \Omega \times Y \tag{10}$$

with n=1,...,n_{dim} and j=1,...,n_{dim}. Considering n_{dim}=3 throughout this Section, the variables of equation (10) read as follows:

- **U**=(v_1,v_2,v_3,p)=(U_m) is the vector of unknowns.

- $\mathbf{A}_n$ is the generalized advection matrix defined as:

$$\mathbf{A}_n = \begin{bmatrix} \rho u_n & 0 & 0 & \delta_{1n} \\ 0 & \rho u_n & 0 & \delta_{2n} \\ 0 & 0 & \rho u_n & \delta_{3n} \\ \delta_{1n} & \delta_{2n} & \delta_{3n} & 0 \end{bmatrix} \tag{11}$$

where δ is the Kronecker symbol. The components of the advection matrix are the coefficients associated with the first derivatives of the unknowns.

• $\mathbf{K}_{jn}$ is the generalized diffusion matrix that can be written as:

$$\mathbf{K}_{jn} = \begin{bmatrix} \mu(\delta_{j1}\delta_{1n} + \delta_{jn}) & \mu\delta_{j2}\delta_{1n} & \mu\delta_{j3}\delta_{1n} & 0 \\ \mu\delta_{j1}\delta_{2n} & \mu(\delta_{j2}\delta_{2n} + \delta_{jn}) & \mu\delta_{j3}\delta_{2n} & 0 \\ \mu\delta_{j1}\delta_{3n} & \mu\delta_{j2}\delta_{3n} & \mu(\delta_{j3}\delta_{3n} + \delta_{jn}) & 0 \\ 0 & 0 & 0 & 0 \end{bmatrix} \tag{12}$$

where the components of the constitutive laws for the deviatoric stress tensor can be clearly identified.

• **M** is the generalized mass matrix:

$$\mathbf{M} = \begin{bmatrix} \rho & 0 & 0 & 0 \\ 0 & \rho & 0 & 0 \\ 0 & 0 & \rho & 0 \\ 0 & 0 & 0 & 0 \end{bmatrix} \tag{13}$$

• $\mathbf{F}=(\rho b_1, \rho b_2, \rho b_3, 0)$ is the generalized force vector.

• $\mathbf{R}=(R_1, R_2, R_3, R_4)$ is the residual vector.

This basic notation is also considered in the description of the upwinding matrix derivation and finite element formulation presented bellow.

The weak form of the convection-diffusion differential system (10) is obtained using a generalized streamline operator (GSO) technique. The resulting variational formulation can be written as [15-17]:

$$\int_{\Omega} \mathbf{N} \cdot \mathbf{R}(\mathbf{U})\, d\Omega + \sum_{n=1}^{n_{el}} \int_{\Omega^{el}} \mathbf{P}(\mathbf{N}) \cdot \mathbf{R}(\mathbf{U})\, d\Omega + \int_{\Gamma} \mathbf{N}_{\mathbf{V}} \cdot [BC]\, \partial\Gamma = 0 \quad \forall \quad \mathbf{N} \in \Phi \tag{14}$$

where Φ is the space of the shape functions **N**. The term BC denotes the proper boundary conditions included in the formulation. In this context, the perturbation function **P**(**N**) is defined as follows:

$$\mathbf{P}(\mathbf{N}) = \boldsymbol{\tau} \cdot (\mathbf{A}_n \nabla_n \mathbf{N}) \tag{15}$$

where $\boldsymbol{\tau}$ is the so-called upwinding matrix. The computation of $\boldsymbol{\tau}$ is performed according to the procedure detailed in [15]. This matrix provides directional upwinding coefficients leading to a non-uniform perturbation function particularly weighted in the required directions. It should be noted that no additional definition for the characteristic element length has to be used and predetermined upwinding coefficients are not required. It is also important to remark that the perturbation function expressed by equation (15) together with the upwinding matrix defined in a unique framework is intended to stabilize the numerical response of the flow problem. In this context, the resulting finite element formulation, identified as FEM3 in the present work, shares all the features of the formulation defined by equation (3).

Finally, the temporal discretization of the unknowns is performed using a Euler backward scheme in the three formulations described above.

3 NUMERICAL SIMULATIONS

The Von-Karman vortex street is studied in the present work for a flow past a cylinder at Reynolds number 100 (based on the cylinder diameter D, i.e., $Re= (D\, U_{in}\, \rho)/\mu$, U_{in} being a characteristic inlet velocity). The geometry analyzed is sketched in Figure 1 showing slip channel walls situated 7 diameters apart from the body of diameter D=2. As previously studied in [6], this configuration leads to results practically independent of the lateral wall distance. The boundary conditions are also included where, in particular, a unit constant velocity profile is adopted as inflow located 7 diameters from the cylinder and, moreover, traction free with zero pressure conditions are considered in the outlet section spaced out 22 diameters from the obstruction. The computations were performed with a finite element mesh composed of 4760 four-noded isoparametric elements (with a fine discretization near the cylinder) and a time step of 0.1 up to a final time of 300.

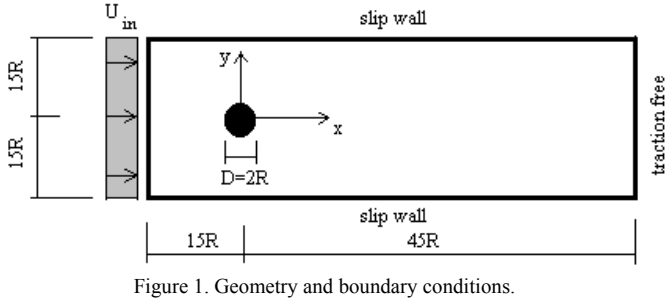

Figure 1. Geometry and boundary conditions.

Although this numerical test was extensively studied by several researchers and reported in

the literature, the present analysis is aimed at studying the following particular features. In order to assess a comparison between the formulations described above, simulations using the FEM1, FEM2 and FEM3 are carried out. The performance of the GMRES and IISD parallel solvers is also tested. Computational time requirements for the codes are evaluated using a interconnected system of personal computers alternatively setting to 1, 2, 3 and 4 nodes. Moreover, the CPU time responses of an improved LU and standard direct solvers, both running in a serial mode, are included for comparison. All the obtained numerical results are compared with those simulations and experiments reported in the literature.

The evolutions of the drag and lift coefficients computed with FEM1 and FEM2 models are shown in Figure 2. Both solutions capture the well-known fact stating that the oscillating period of the drag coefficient is approximately twice of that corresponding to the lift coefficient and provide similar amplitudes for these evolutions.

Figures 3 to 5 respectively depicts time histories for the x and y velocity components and pressure at four points positioned at x=2.0, x=7.9, x=40.2 and x=45.0, simulated once again with FEM1 and FEM2 formulations. A very good agreement between both results can be observed. Moreover, these predictions verify the numerical behavior described in [2] where, in particular, the y-component of the velocity oscillates with a period similar to that of the lift coefficient while the other variables (x-component of the velocity and pressure) behave in time as the drag coefficient. It is important to remark that the results obtained do not exhibit a high dependency of the outlet boundary conditions. To test this, pressure-free conditions were also considered (results not shown) giving very similar results to those already presented in Figures 2 to 5.

Table 1 shows computed mean drag value and amplitude of the lift coefficient in a reasonably good comparison with those reported in the literature for similar geometric configurations and space/time discretizations.

Additionally, simulations with the FEM1 model using one and four Newton-Raphson iterations (nnwt=1 and 4 where convergence is achieved for this last value) are presented in Figure 6 in order to illustrate the numerical effects of the iterative procedure in the numerical response. A large difference between both numerical strategies can be observed in the evolution of the drag and lift coefficients. Nevertheless, this discrepancy is within the dispersion of values shown in Table 1.

Computational times required for the analysis are summarized in Table 2 for one or multi processor simulations using different solvers. The resulting speedups for 2, 3 and 4 processors are 1.7, 2.2 and 2.8, respectively. The time comparison for solvers GMRES and IISD is in particular relevant due to their parallel capabilities. Furthermore, the CPU time consumed by the serial code is lower to that required by the GMRES running in one processor but, however, is substantially larger than that corresponding to the IISD and improved LU solvers. Finally, the similar performance exhibit by the FEM2 and FEM3 models reflects the relative smallness of the computational effort needed to compute the more complex perturbation function of the latter formulation.

Table 1. Comparison of mean drag value and amplitude of the lift coefficient.

	Mean drag coefficient	Amplitude of the lift coefficient
Present work – FEM1	1.362	0.257
Present work – FEM2	1.370	0.264
Present work – FEM3	1.363	0.278
Behr et al. [6] – STVP	1.384	0.374
Behr et al. [6] – VPS	1.403	0.369
Engelman and Jamnia [2]	1.411	0.350
Tezduyar and Liou [5]	1.393	0.312
Tabata amd Fujima [13]	1.350	0.300
Mittal and Tezduyar [14]	1.382	0.350
Tezduyar et al. [4] – Q1Q1/T1	1.387	0.370
Tezduyar et al. [4] – Q1Q1/T6	1.400	0.370
Tezduyar et al. [4] – P1P1/T1	1.380	0.374
Tezduyar et al. [4] – P1P1/T6	1.394	0.375
Piñol and Grau [7] – F1	1.325	0.268
Piñol and Grau [7] – F2	1.325	0.240
Piñol and Grau [7] – F3	1.325	0.240
Zhang et al. [9]	1.430	0.255
Beaudan and Moin [10]	1.320	0.340
Li et al. [11]	1.332	0.360
Braza et al. [1]	1.270	0.300
Henderson [12] – numerical correlation	1.355	------
Tritton [26] – experimental	1.260	------
Wieselsberger [27] – experimental	1.430	------
Tanida et al. [28] – experimental	------	0.075
Tritton [29] – experimental correlation	1.270	------

Table 2. CPU times in minutes.

	1 processor	2 processors	3 processors	4 processors
FEM1 - GMRES	2758	1585	1226	985
FEM1 - IISD	751	439	342	268
FEM1 - LU	543	------	------	------
FEM2 - DIRECT	1816	------	------	------
FEM3 - DIRECT	1886	------	------	------

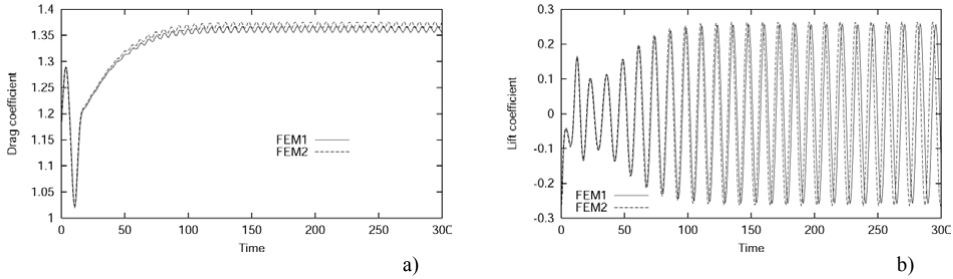

a) b)

Figure 2. Time histories of a) drag and b) lift coefficients.

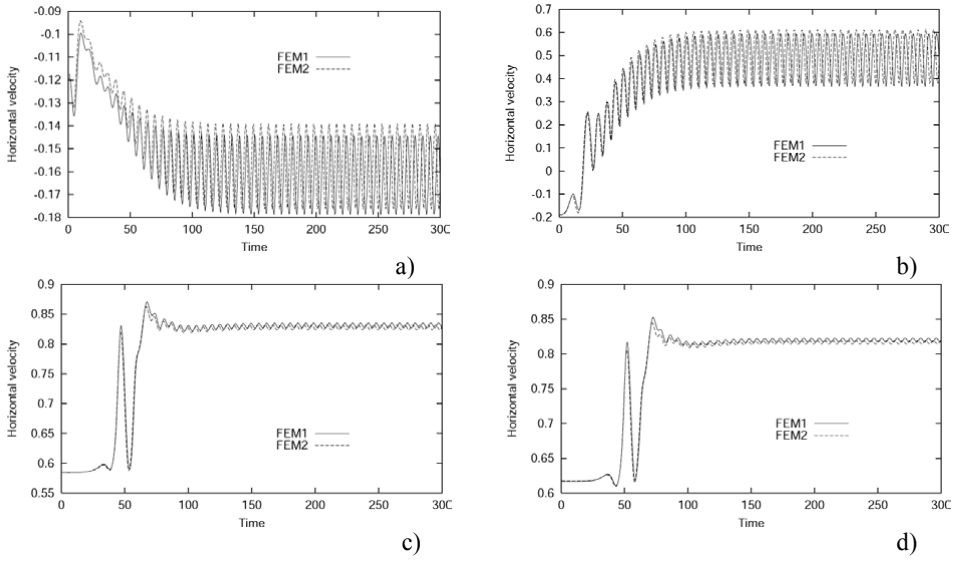

Figure 3. Time histories of the horizontal velocity at points located at a) x=2.0, b) x=7.9, c) x=40.2 and d) x=45.0.

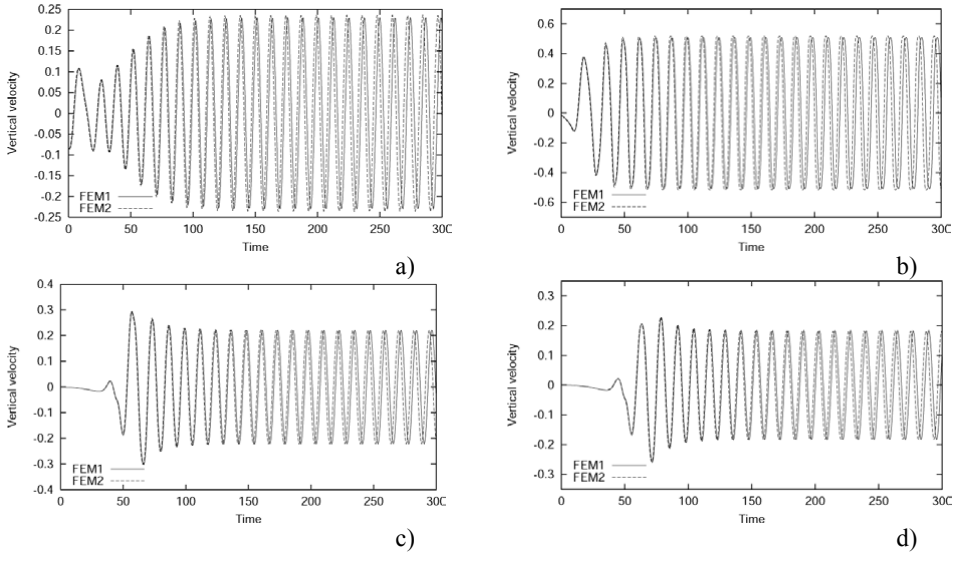

Figure 4. Time histories of the vertical velocity at points located at a) x=2.0, b) x=7.9, c) x=40.2 and d) x=45.0.

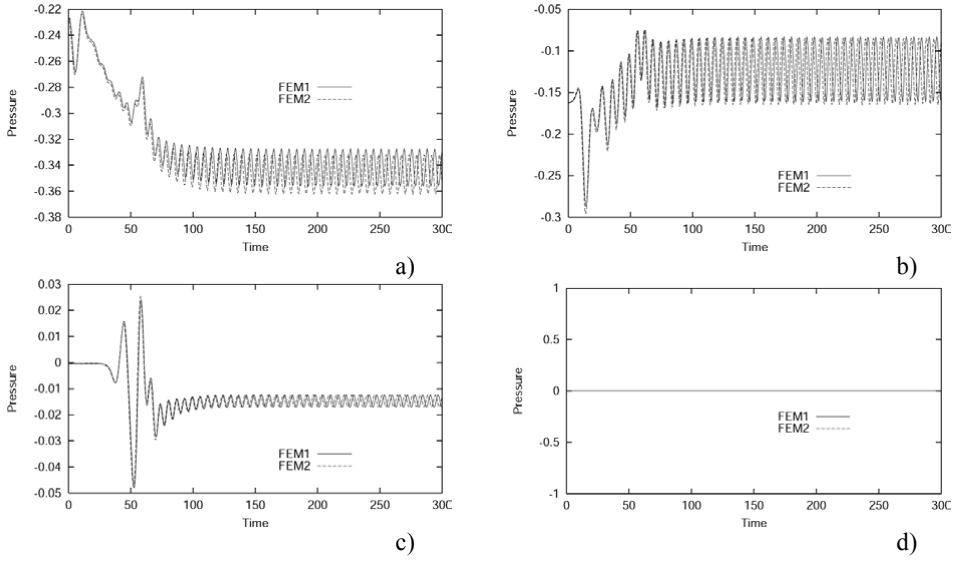

Figure 5. Time histories of the pressure at points located at a) x=2.0, b) x=7.9, c) x=40.2 and d) x=45.0.

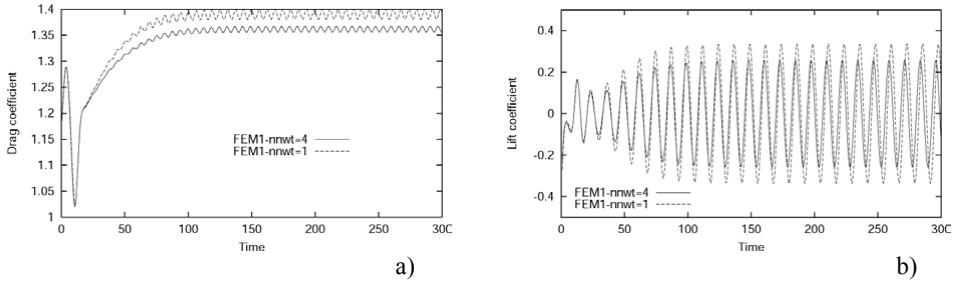

Figure 6. Time histories of a) drag and b) lift coefficients for different convergence strategies.

4 CONCLUSIONS

A comparative assessment of different methodologies have been presented in the numerical simulations of past cylinder flows for Re=100. In particular, this study has encompassed the performance analysis of three incompressible Navier-Stokes formulations running in serial and parallel contexts with several solvers.

The numerical predictions obtained in this work reasonably fit the available results

reported in the literature. Moreover, the evaluation of CPU requirements showed a good behavior of the installed interconnected system of four personal computers where efficient capabilities of the optimized IISD solver were ratified.

Acknowledgments

The supports provided by the Andes Foundation Chile under project "Parallel computation of mechanical problems using an interconnected system of personal computers" (Argentinean-Chilean Scientific-Academic Cooperation Program, 2001/2002) and the Department of Technological and Scientific Research at the Universidad de Santiago de Chile are gratefully acknowledged.

5 REFERENCES

[1] Braza M., Chassaing P. and Ha Minh H.: "Numerical study and physical analysis of the pressure and velocity fields in the near wake of a circular cylinder", *J. Fluids Mechanics*, Vol. 165, pp. 79-130 (1986).

[2] Engelman M.S. and Jamnia M-A.: "Transient flow past a circular cylinder: a benchmark solution", *Int. J. Numerical Methods in Fluids*, Vol. 11, pp. 985-1000 (1990).

[3] Tezduyar T. E., Behr M., Mittal, S. and Johnson A.A.: "Computation of unsteady incompressible flows with the stabilized finite element methods: space-time formulations, iterative strategies and massively parallel implementations", *New Methods in transient Analysis*, PVP-Vol. 246/AMD-Vol. 143, pp. 7-24 (1992).

[4] Tezduyar T. E., Mittal S., Ray S.E. and Shih R.: "Incompressible flow computations with stabilized bilinear and linear equal-order-interpolation velocity-pressure elements", *Computer Methods in Applied Mechanics and Engineering*, Vol. 95, pp. 221-242 (1992).

[5] Tezduyar T.E. and Liou J.: "On the downstream boundary conditions for the vorticity-stream function formulation of two-dimensional incompressible flows", *Computer Methods in Applied Mechanics and Engineering*, Vol. 85, pp. 207-217 (1991).

[6] Behr M., Hastreiter D., Mittal S. and Tezduyar T. E.: "Incompressible flow past a circular cylinder: dependence of the computed flow field on the location of the lateral boundaries", *Computer Methods in Applied Mechanics and Engineering*, Vol. 123, pp. 309-316 (1995).

[7] Piñol S. and Grau F. X.: "Influence on the no-slip boundary condition on the prediction of drag, lift, and heat transfer coefficients in the flow past a 2-D cylinder", *Numerical Heat Transfer, part A*, Vol.34, 313-330 (1998).

[8] Guo T., Chew Y.T., Luo S.C. and Su M.D.: "A new numerical simulation method of high Reynolds number flow around a cylinder", *Computer Methods in Applied Mechanics and Engineering*, Vol. 158, pp. 357-366 (1998).

[9] Zhang H.Q., Fey U., Noack B.R., König M. and Eckelmann H.: "On the transition of the cylinder wake", *Phys. Fluids*, Vol. 7, No. 4, 779-794 (1995).

[10] Beaudan P. and Moin P.: "Numerical experiments on the flow past a circular cylinder at

subcritical Reynolds number", Report TF-62, Stanford University (1994).
[11] Li J., Chambarel A., Donneaud M. and Martin R.: "Numerical study of laminar flow past one and two circular cylinders", *Comput. Fluids*, Vol. 19, No. 2, 155-170 (1991).
[12] Henderson R.D.: "Details of the drag curve near the onset of vortex shedding", *Phys. Fluids*, Vol. 7, No. 9, 2102-2104 (1995).
[13] Tabata M. and Fujima S.: "An upwind finite element scheme for high-Reynolds-number flows", *International Journal for Numerical Methods in Fluids*, Vol. 12, pp.305-322 (1991).
[14] Mittal S. and Tezduyar T.E.: "Notes on the stabilized space-time finite-element formulation of unsteady incompressible flows", *Computer Physics Communications*, Vol. 73 , pp. 93-112 (1992).
[15] Storti M., Nigro N. and Idelsohn S.: "Stability analysis of mixed finite element formulations with special mention to stabilized equal-order interpolations", *International Journal for Numerical Methods in Fluids*, Vol. 20, pp.1003-1022 (1995).
[16] Storti M., Nigro N. and Idelsohn S.: "Equal-order interpolations: a unified approach to stabilize the incompressible and convective effects". *Computer Methods in Applied Mechanics and Engineering*, Vol. 143, pp. 317-331 (1997).
[17] Cruchaga M.A. and Oñate E: "A finite element formulation for incompressible flow problems using a generalized streamline operator", *Computer Methods in Applied Mechanics and Engineering*, Vol. 143, pp. 49-67 (1997).
[18] Cruchaga M.A.: "A study of the backward-facing step problem using a generalized streamline formulation", *Communications in Numerical Methods in Engineering*, Vol. 14, pp. 697-708 (1998).
[19] Cruchaga M.A. and Oñate, E: "A generalized streamline finite element approach for the analysis of incompressible flow problems including moving surfaces", *Computer Methods in Applied Mechanics and Engineering*, Vol. 173, pp. 241-255 (1999).
[20] Cruchaga M.A. and Oñate E.: "A numerical solution strategy for the incompressible Navier-Stokes equations", Proceedings of the Conference of Modelling and Simulation, pp. 699-703 (1994).
[21] Mittal S. and Tezduyar T.E.: "Massively parallel finite element computation of incompressible flows involving fluid-body interactions", *Computer Methods in Applied Mechanics and Engineering*, Vol. 112, pp. 253-282 (1994).
[22] Behr M. and Tezduyar T.E.: "Finite element solution strategies for large-scale flow formulations", *Computer Methods in Applied Mechanics and Engineering*, Vol. 112, pp. 3-24 (1994).
[23] Nigro N. and Storti M.: Internal Report, CIMEC (2000). See also: http://minerva.arcride.edu.ar/petscfem
[24] Storti M., Nigro N. and Idelsohn S.: "GMRES physics based preconditioner for all Reynolds and Mach number. Numerical examples", *International Journal for Numerical Methods in Fluids*, Vol. 25, pp. 1-25 (1997).
[25] Nigro N., Storti M., Idelsohn S. and Tezduyar T.; "Physics based GMRES preconditioner for compressible and incompresssible Navier-Stokes equations", *Computer Methods in*

Applied Mechanics and Engineering, Vol. 154, pp. 203-228 (1998).
[26] Tritton D.J.: "Experiments on the flow past a circular cylinder at low Reynolds numbers", *J. Fluid Mech.*, Vol. 6, part 4, 547-567 (1959).
[27] Wieselsberger C. Von: "Neuere Festellungen über die Gesetze des Flüssigkeits un Luftwiderstands", *Phys. Z.*, Vol. 22, 321-328 (1921).
[28] Tanida Y., Okajima A. and Watanabe Y.: "Stability of a circular cylinder oscillating in uniform flow or in a wake", *J. Fluid Mech.*, Vol. 61, 769-784 (1973).
[29] Tritton D.J.: *Physical Fluid Dynamics*, 2nd ed., Clarendon Press, Oxford (1989).